JOURNAL OF GUIDANCE, CONTROL, AND DYNAMICS
Vol. 19, No. 1, January–February 1996

Four-Dimensional Guidance of Atmospheric Vehicles

Ilie Stiharu-Alexe and Jules O'Shea
École Polytechnique de Montréale, Montréal H3C 3A7, Canada

The nonlinear control theories based upon the model predictive control and the nonlinear inverse control are used to develop four-dimensional guidance controllers, the conversion of the primary trajectory being assumed by a specific solution to the inverse kinematics problem. The control task is simplified by using the forced singular perturbation theory, overall system dynamics being separated into the fast and slow reduced-order systems and separately controlled. The algorithm performances are evaluated in the case of a conventional transport aircraft that tracks a four-dimensional trajectory defined by flight levels, waypoints, and an estimated time of arrival. The predictive control and dynamic inversion are compared as basic algorithms for the fast-dynamics control in view of establishing performances and limits.

Nomenclature

a_N, a_E, a_D	= inertial acceleration components
b, c	= aerodynamic chord, wing span
$C_{(\cdot)}$	= nondimensional force coefficients
F_x, F_y, F_z	= aerodynamic forces in body frame
g	= acceleration of gravitation
I_x, I_y, I_z, I_{xz}	= moments and product of inertia
L, M, N	= roll, pitch and yaw moments
m	= vehicles mass
P, Q, R	= roll, pitch, and yaw rates in body frame
R_N, R_E, R_D	= inertial position coordinates (north, east, and down, respectively)
S	= equivalent surface
U, V, W	= velocity components in body frame
V_N, V_E, V_D	= inertial velocity components
α	= angle of attack
β	= sideslip angle
$\Delta_{(\cdot)}$	= atmospheric vehicle controls
ρ	= air density
Φ, Θ, Ψ	= roll, pitch, and yaw attitudes

Subscripts

B	= body reference
I	= inertial reference
W	= wind reference

Superscripts

C	= corrected value
D	= desired value

I. Introduction

WITH the advent of the Global Navigation Satellite System (GNSS), four-dimensional (a time-defined three-dimensional trajectory) tracking will constitute a typical task for the coming generation of atmospheric vehicle autopilots that will ensure all authority guidance. For helicopters, for which the dominant force controls vertical direction, Ref. 1 presents a thorough study of four-dimensional guidance, introducing time separation, a particular solution of the inverse kinematics problem, and the control of the fast dynamics by use of a nonlinear transformation. In a more general case of an atmospheric vehicle, as in the airplane case, where the dominant force controls two directions, the problem of controlling translational motion cannot be solved so directly. Further development is required to obtain a more general method of control applicable to all atmospheric vehicles, helicopters, and airplanes.

Ilie Stiharu-Alexe received a Ph.D. degree in Aeronautical Engineering from the Polytechnic University of Bucharest, Romania, in 1982 and a graduate degree in Electrical Engineering (Avionics) in 1975. Since 1979, he has been on the faculty of the Polytechnic University of Bucharest, where he is an Associate Professor of Aeronautics. After a postdoctoral term in the Automatics Laboratory of Grenoble, he is currently an Associate Researcher at the Electrical and Computer Engineering Department of the Polytechnic School of Montreal. Stiharu-Alexe's interests include computer simulation, robust and nonlinear control, and avionics. He is an AIAA member.

Jules O'Shea graduated from Ecole Polytechnique of Montreal in 1957, where he obtained a B.A.Sc. degree in Electrical Engineering. He then worked for Canadair and later for Boeing in the field of electrohydraulic servos. In 1966, he became a research engineer at the LAAS in Toulouse, France. He obtained a Doctor-Engineer degree from the University of Toulouse in 1971. Then he joined the Electrical and Computer Engineering Department of École Polytechnique de Montréale as Assistant Professor. In 1974, he was promoted to the rank of full Professor and later he became head of the department. He is now responsible for the Graduate Program in Aerospace of his department. He is an AIAA member.

Received Nov. 12, 1993; revision received April 6, 1995; accepted for publication June 2, 1995.

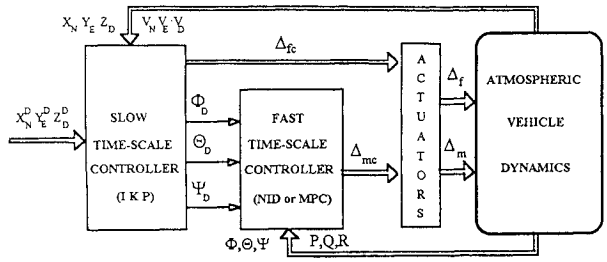

Fig. 1 Atmospheric vehicle guidance block diagram.

The desired four-dimensional trajectory results either from the flight plan (comprising the desired flight levels, waypoints, and times of arrival) or from the solution of the kinematics mass-point optimization problem in the case of more specialized maneuvers. The precise tracking of that trajectory requires a high-performance control system. To that end, one can take advantage of methods such as the predictive control or the nonlinear inversion control, which will be specifically studied in this paper. To keep the airplane model rigorous, the nonlinear model proposed in Refs. 2–5 (developed from the classical references 6–8) seems particularly well suited. Obviously one then encounters the inverse kinematics problem (IKP). Reference 1 dealt with IKP for the helicopter case, but it will be derived differently in this paper in the airplane case. In Ref. 2, the nonlinear dynamic inversion method is used to control a supermaneuverable aircraft acting in a different way on the fast and slow dynamics. This paper proposes a four-dimensional guidance control algorithm based on an IKP solution for the slow dynamics and a nonlinear inverse dynamics/model predictive control (NID/MPC) solution for the fast dynamics. Many noticed, as in Refs. 1–5 and 9, that the time constants associated with the translational motion usually exceed by one order of magnitude those associated with the rotational motion. Hence it leads to the separation of slow and fast state variables, allowing one to obtain a reduction of the system order. Indeed the small perturbation theory lends itself very well for solving the aircraft control problem.

In this study, the authors propose to control the fast dynamics by adapting either the general MPC strategy,[10–13] combined with a specific method of local dynamics state estimation and identification,[14] or the NID control method,[15–17] both leading to interesting results. These general control algorithms were adapted to the case of atmospheric vehicles by defining the state and output variables in such a way as to make them more accessible and also to facilitate the tuning of the parameters. This tuning process was performed by means of a complete set of simulations until the right transient and steady-state performances were obtained. For the slow time-scale part of the system, the inverse kinematics problem is solved assuming the atmospheric vehicle is not on the desired trajectory. Thus one obtains an algorithm that uses the four-dimensional trajectory, the desired attitude pseudocontrols Φ^D, Θ^D, Ψ^D, and a differential thrust (Δ_f) command. In turn, the desired attitude pseudocontrols become the reference inputs to the fast dynamics. Applying then the inverse kinematics scheme, one gets a reference for the thrust and the attitude. Therefore, the proposed algorithm permits, at the level of the fast time-scale dynamics, the full control of the vehicle velocity vector: its magnitude being thrust dependent and its orientation being determined by the vehicle attitude. The fast dynamics is controlled by high-performance nonlinear algorithms, and this allows a very precise tracking as confirmed by means of simulation. To be realistic, the system simulation includes models for servo and acquisition elements and takes into account the speed and amplitude saturation as well as the atmospheric disturbance using the Dryden model and the transient-analog equivalence. Figure 1 sums up the proposed control scheme for the four-dimensional guidance of an atmospheric vehicle.

II. Vehicle Model

In this study, one considers the guidance of an atmospheric vehicle problem for a medium-time flight duration. So, one can adapt the flat-Earth assumption and use the six-degree-of-freedom rigid-body vehicle model. This allows one to write the well-known equations describing translation[6,7]

$$\begin{pmatrix}\dot{R}_N\\ \dot{R}_E\\ \dot{R}_D\end{pmatrix} = \begin{pmatrix}V_N\\ V_E\\ V_D\end{pmatrix} = L_{IB}\begin{pmatrix}U\\ V\\ W\end{pmatrix} \tag{1}$$

$$\begin{pmatrix}\dot{V}_N\\ \dot{V}_E\\ \dot{V}_D\end{pmatrix} = L_{IB}\begin{pmatrix}f_x\\ f_y\\ f_z\end{pmatrix} + \begin{pmatrix}0\\ 0\\ g\end{pmatrix} \tag{2}$$

where

$$f_x = F_x/m, \quad f_y = F_y/m, \quad f_z = F_z/m \tag{3}$$

and $L_{IB}(-\Phi, -\Theta, -\Psi)$ represents the body-to-inertial frame transformation matrix.

The vehicle attitude (rotational) dynamics can be represented by

$$\begin{pmatrix}\dot{P}\\ \dot{Q}\\ \dot{R}\end{pmatrix} = \begin{pmatrix}\left(E_p I_z + E_r J_{xz}\right)/\left(I_x I_z - J_{xz}^2\right)\\ \left(M + J_{xz}(R^2 - P^2) + (I_z - I_x)PR\right)/I_y\\ \left(E_r I_x + E_p J_{xz}\right)/\left(I_x I_z - J_{xz}^2\right)\end{pmatrix} \tag{4}$$

$$E_p = J_{yz}PQ - (I_y - I_z)QR + L \tag{5}$$

$$E_r = -J_{xy}QR + (I_x - I_y)PQ + N \tag{6}$$

and the angular velocities relative to the inertial frame can be obtained by the transformation

$$\begin{pmatrix}\dot{\Phi}\\ \dot{\Theta}\\ \dot{\Psi}\end{pmatrix} = \begin{pmatrix}1 & \sin\Phi\tan\Theta & \cos\Phi\tan\Theta\\ 0 & \cos\Phi & -\sin\Phi\\ 0 & \sin\Phi\sec\Theta & \cos\Phi\sec\Theta\end{pmatrix}\begin{pmatrix}P\\ Q\\ R\end{pmatrix} \tag{7}$$

III. Control Strategy

For reducing the large 12th-order model given by Eqs. (1–7), one resorts to the singular perturbation theory so as to obtain two subsystems, one with slow and the other with fast dynamics.[2–5] Assuming the separation between the force- and moment-generating phenomena and knowing that the time constants associated with the translational dynamics are long compared with the rotational dynamics, one takes Eqs. (1–3) as the slow subsystem and Eqs. (4–7) as the fast subsystem. This leads to the following state-space formulation:

$$\dot{\boldsymbol{X}} = \boldsymbol{F}(\boldsymbol{X}, \boldsymbol{U}) \tag{8}$$

where $\boldsymbol{X} = (X_S\ X_F)^T$ and $\boldsymbol{U} = (U_S\ U_F)_F^T$. Equation (8) is imbedded in the equations

$$\dot{X}_S = f(X_S, X_F, U_S, \epsilon U_F, \epsilon) \tag{9}$$

$$\epsilon\dot{X}_F = g(X_S, X_F, U_S, \epsilon U_P, \epsilon) \tag{10}$$

where ϵ is the singular perturbation theory small parameter and $X_S^T = (R_N, R_E, R_D, V_N, V_E, V_D)$ represents the slow time-scale state vector, $X_F^T = (\Phi, \Theta, \Psi, \dot{\Phi}, \dot{\Theta}, \dot{\Phi})$ the fast time-scale one, and $\boldsymbol{U}$ the vehicle command as $\boldsymbol{U} = (\Delta_f, \Delta_m)^T$ with force $\Delta_f = \Delta_T$ and moment $\Delta_m = (\Delta_L, \Delta_M, \Delta_N)^T$ components. To describe the slow time-scale dynamics, the parameter ϵ is set to zero. Equation (10) becomes $g(\bar{X}_S, \bar{X}_F, \bar{U}_S, 0, 0) = 0$, being solved algebraically for $\bar{X}_F$ as a function of $\bar{X}_S$ and $\bar{U}_S$, the slow time-scale state and control:

$$\bar{X}_F = G(\bar{X}_S, \bar{U}_S) \tag{11}$$

This procedure reduces the dynamic part to the slow subsystem with the slow time-scale state and control:

$$\dot{\bar{X}}_S = f(\bar{X}_S, G(\bar{X}_S, \bar{U}_S), \bar{U}_S, 0) = F(\bar{X}_S, \bar{U}_S) \tag{12}$$

Interpreting Eq. (11), one must conclude that the fast subsystem responds so quickly that its transients die out instantaneously. Solving the fast time-scale problem, with $\bar{\Phi} = \bar{\Theta} = \bar{\Psi} = 0$, the resulting values $\bar{\Phi}, \bar{\Theta}, \bar{\Psi}$, designate the slow time-scale desired body attitudes Φ^D, Θ^D, Ψ^D. Thus the only control considered here is the force-generating control $\bar{U}_S = \Delta_f$. Meanwhile, at the same level, the steady-state values of the attitudes Φ^D, Θ^D, Ψ^D appear as pseudocontrols for the fast time scale system. The fundamental assumption that justifies this approach comes from the fact the vehicle has attained the moment equilibrium at the slow time scale, the moment generated by the control Δ_f being trimmed by the moment-generating devices. In the fast time scale, the slow states are assumed to be known constant values, resulting in the solution of the inverse kinematics problem.

IV. Slow Time-Scale IKP Algorithm

The slow time-scale system is designed to track the position coordinates $\bar{R}^D(R_N^D, R_E^D, R_D^D)$ of the desired four-dimensional trajectory, which results from a spline interpolation over the desired waypoint at the desired flight levels or from a kinematics mass-point optimization. A specific requirement for high-performance tracking, according to the vehicle class, is that the maximum vehicle acceleration on the trajectory does not exceed the values imposed by the admissible load factor (ALF).[17] To comply with this requirement at the level of the slow time-scale system, the reference acceleration converted into the body axes is bounded to a value limited by the ALF (Fig. 2).

The main task of the slow time-scale IKP algorithm is to supply the steady-state attitudes $\bar{\Phi}, \bar{\Theta}, \bar{\Psi}$ and the force-generating control Δ_f. To accomplish this, the left side of Eq. (2) is replaced by the desired acceleration vector [Eq. (13)] resulting from the desired trajectory. At this level, the steady-state values of the body Euler angles are used in the computation of the L_{IB} matrix:

$$\boldsymbol{a}^D = \begin{pmatrix} \boldsymbol{a}_N^D \\ \boldsymbol{a}_E^D \\ \boldsymbol{a}_D^D - g \end{pmatrix} = L_{IB} \begin{pmatrix} f_x \\ f_y \\ f_z \end{pmatrix} = L_{IB}\boldsymbol{f} \tag{13}$$

One must solve Eq. (13) in order to find the $\bar{\Phi}, \bar{\Theta}, \bar{\Psi}$ that represent the IKP solution. Since L_{IB} is purely a rotation transformation, the magnitude of the desired acceleration vector $\boldsymbol{a}^D$ and the body specific force $\boldsymbol{f}$ must be equal in order to find a solution for the Euler angles. The force-generating control Δ_f is then used to adjust the magnitude of the forces acting on the body (which modifies the vehicle speed magnitude) to assure the equality from Eq. (13).

The solution of the IKP relies on the factorization

$$L_{IB} = L_{BW}L_{WI} \tag{14}$$

where $L_{WI}(\Psi_w, \Theta_w, \Phi_w)$ is the inertial-to-wind transformation matrix and $L_{BW}(0, -\alpha, \beta)$ is the wind-to-body transformation matrix. Exploiting the fact that all aerodynamic forces are primarily expressed in the wind frame, Eq. (13) may be rewritten in a more adequate form for this application[9]:

$$L_{IW}\boldsymbol{a}^D = \boldsymbol{f}_w = (f_{xw}, f_{yw}, f_{zw})^T \tag{15}$$

At this point Eq. (15) contains five unknowns, $\Theta_w, \Psi_w, \Phi_w, f_{xw}$, and f_{zw}, with the assumption that the lateral force in the aerodynamic reference is not affected by the force-generating control Δ_f. Although f_{xw} and f_{zw} are strictly related to the angle of attack α and the control Δ_f, f_{yw} can be considered with its current value

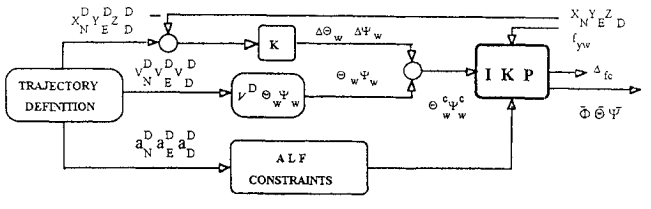

Fig. 2 IKP solution block diagram.

obtained either from the aerodynamic model or from the sensed accelerations and angular velocities of the vehicle.

If the atmosphere is assumed to be at rest, which is a reasonable hypothesis for the medium-time intervals between acquisitions, the desired inertial velocity components can be related to the desired airspeed V^D, heading Ψ_w, and flight-path angle Θ_w by

$$V^D = \left(V_N^{D^2} + V_E^{D^2} + V_D^{D^2}\right)^{\frac{1}{2}} \tag{16}$$

$$\Theta_w = \sin^{-1}\left(V_D^D / V^D\right) \tag{17}$$

$$\Psi_w = \tan^{-1}\left(V_E^D / V_N^D\right) \tag{18}$$

Equations (15–18) have been written with respect to the desired trajectory, i.e., the desired acceleration and speed. Considering the fact that in the course of tracking the vehicle may not be on the desired trajectory (but is sufficiently near), an elementary feedback follower was designed to minimize the tracking error using the proportional navigation criterion.[9] This has been implemented using the tracking error expressed by LD, the lateral deviation with respect to the wind frame, and VD, the vertical deviation:

$$\mathrm{LD} = -\left(R_N^D - R_N\right)\sin\Psi_w + \left(R_E^D - R_E\right)\cos\Psi_w \tag{19}$$

$$\mathrm{VD} = R_D^D - R_D \tag{20}$$

Thus, before using Eq. (15), the heading Ψ_w and the flight-path angle Θ_w are converted to Ψ_w^c and Θ_w^c according to the proportional law:

$$\Psi_w^c - \Psi_w = \Delta\Psi_w = K_L\mathrm{LD} \tag{21}$$

$$\Theta_w^c - \Theta_w = \Delta\Theta_w = K_V\mathrm{VD} \tag{22}$$

where K_L, K_V are linear feedback gains.

Then equating the three components of Eq. (15) yields

$$a_N^D\cos\Theta_w^c\cos\Psi_w^c + a_E^D\cos\Theta_w^c\sin\Psi_w^c - a_D^D\sin\Theta_w^c = f_{xw} \tag{23}$$

$$a_N^D\left(\sin\Phi_w\sin\Theta_w^c\cos\Psi_w^c - \cos\Phi_w\sin\Psi_w^c\right) + a_E^D\left(\sin\Phi_w\sin\Theta_w^c\sin\Psi_w^c + \cos\Phi_w\cos\Psi_w^c\right) + a_D^D\sin\Phi_w\cos\Theta_w^c = f_{yw} \tag{24}$$

$$a_N^D\left(\cos\Phi_w\sin\Theta_w^c\cos\Psi_w^c + \sin\Phi_w\sin\Psi_w^c\right) + a_E^D\left(\cos\Phi_w\sin\Theta_w^c\sin\Psi_w^c - \sin\Phi_w\cos\Psi_w^c\right) + a_D^D\cos\Phi_w\cos\Theta_w^c = f_{zw} \tag{25}$$

In addition to components related to the desired acceleration on the trajectory, the left-hand side of Eqs. (23–25) includes also small corrections due to the instantaneous rotation on the transient comeback trajectory. In conjunction with Φ_w from Eq. (24), Eqs. (23–25) can be used to determine the f_{xw} and f_{zw} force components. Considering simplified representations for the aerodynamic forces, the angle of attack α and the force-generating control Δ_f can be easily computed as functions of the current flight conditions.[4,9] This is a general solution that covers the case of the helicopters.[1]

Assuming that the vehicle must track the trajectories with zero sideslip, i.e., $\beta = 0$, an analytical solution for the steady-state attitudes is then supplied based upon Eq. (14):

$$\bar{\Theta} = \sin^{-1}\left(\sin\Theta_w^c\cos\alpha + \cos\Phi_w\cos\Theta_w^c\sin\alpha\right) \tag{26a}$$

$$\bar{\Phi} = \sin^{-1}\left[\left(\sin\Phi_w\cos\Theta_w^c\right)/\cos\bar{\Theta}\right] \tag{26b}$$

$$\bar{\Psi} = \sin^{-1}\left\{\left[\cos\Theta_w^c\cos\Psi_w^c\cos\alpha - \left(\cos\Phi_w\sin\Theta_w^c\cos\Psi_w^c + \sin\Phi_w\sin\Psi_w^c\right)\sin\alpha\right]/\cos\bar{\Theta}\right\} \tag{26c}$$

Thus, the solution to the inverse problem of flight mechanics makes possible the computation of the force-generating control Δ_f and

the pseudocontrols $\bar{\Phi}$, $\bar{\Theta}$, $\bar{\Psi}$ as desired attitudes to be tracked at the fast time-scale level. The slow time-scale parameters depend on the fast dynamics control, the computation of the desired attitude being dependent of the current position and attitude of the vehicle. This dependence may be controlled by the selection of the feedback gains and represents one of the tuning steps.

V. Fast Time-Scale Algorithm

The fast time-scale tracking algorithm assures, based upon an NID or an MPC approach, the pursuit of the desired attitudes $\bar{\Phi}$, $\bar{\Theta}$, $\bar{\Psi}$, obtained as a solution of the IKP. The selection of an adequate approach depends on the required performances as well as on the available information to be measured during the tracking process. The NID approach, though easy to implement, causes the deterioration of the tracking performances because of the modeling imperfections that generate dynamic errors.[9] The algorithm performance may be improved by parameter estimation, thus increasing algorithm complexity and effectiveness. In the most common tracking maneuvers, transport vehicles use the basic NID algorithm. In the case of an on-line identified model and trajectory prediction over the adequate time horizon, the MPC approach assures very good tracking performance but is difficult to implement due to the requirement for large memory and computational speed.[14,17] This type of solution may be necessary if a very precise four-dimensional tracking is required. In the following section a practical implementation of these two approaches is presented for the case of conventional aircraft, as well as considerations pertaining to helicopters.

A. NID Tracking Algorithm

NID Mathematical Formulation

Figure 3 presents the control configuration block diagram of the fast time-scale system based on slightly modified NID differentiation technique[16] in the sense that a particular set of state and output variables was selected to include variables related to either global or inertial navigation. For this approach the fast system dynamics is modeled as in Eqs. (27) and (28):

$$\dot{X}_F = A(X_F) + B(X_F)\Delta_m \tag{27}$$

$$Y_F = C_F X_F \tag{28}$$

where $Y_F = [\Phi, \Theta, \Psi]^T$ represents the controlled state and Δ_m represents the control vector, defined as $\Delta_m = [\Delta_e, \Delta_a, \Delta_r]^T$ for the conventional aircraft with elevator, aileron, and rudder controls or for helicopters with lateral cyclic stick, longitudinal cyclic stick, and directional control.

As required by the differential NID technique, the controlled states are successively differentiated until control terms appear.[15,16] In this case differentiating twice will suffice. The result can be written in a compact form:

$$Y_F^{(2)} = A^*(X_F) + B^*(X_F)\Delta_m \tag{29}$$

with $Y_F^{(2)}$ the second-order derivative of the output vector and $A^*(\cdot)$, $B^*(\cdot)$ as defined in Ref. 4.

A sufficient condition for the existence of an inverse system model to Eqs. (27) and (28) is that B^* in Eq. (29) be nonsingular.[16,17] In this case, the inverse system model takes the form

$$\dot{X}_F = [A(X_F) - B(X_F)F(X_F)] + B(X_F)G(X_F) \tag{30}$$

$$\Delta_m = -F(X_F) + G(X_F)v \tag{31}$$

where $v = Y_F^{(2)}$ represents the input of the inverse system and Δ_m represents the output, with the matrices $G(X_F) = [B^*(X_F)]^+$ and

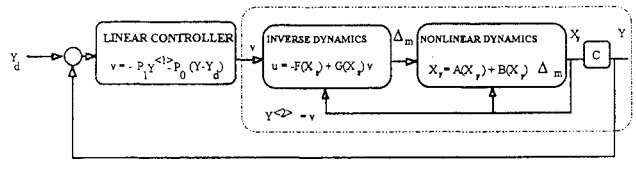

Fig. 3 NID solution block diagram.

$F(X_F) = [B^*(X_F)]^+ A^*(X_F)$, $(\cdot)^+$ being the pseudoinverse of the matrix. Applying the NID control law [Eq. (31)] to the original system of Eqs. (27) and (28) leaves it in the integrator-decoupled form $Y_F^{(2)} = v$. Setting v as the output of a compensator dynamics of the form presented in Eq. (32) gives the original system the decoupled linear, time-invariant dynamics [Eq. (33)]:

$$v = -P_1 Y_F^{(1)} - P_0\left(Y_F - Y_F^D\right) \tag{32}$$

where P_k can be selected as constant diagonal matrices:

$$Y_F^{(2)} + P_1 Y_F^{(1)} + P_0 Y_F = P_0 Y_F^D \tag{33}$$

where $Y_F^D = (\bar{\Phi}, \bar{\Theta}, \bar{\Psi})^T = (\Phi^D, \Theta^D, \Psi^D)^T$ represents the attitude pseudocontrols.[4,9]

NID Implementation

The atmospheric vehicle equations of motion (Sec. III) can be organized into triangular form[4,16]:

$$\dot{X}_{F1} = A_1(X_{Fi}) + B_1(X_{Fi})U_{F1} \qquad i = 1, 3 \tag{34}$$

$$\dot{X}_{F2} = A_2(X_{Fi}, U_{Fj}) + B_2(X_{Fi}, U_{Fj})U_{F2}$$

$$i = 1, 3;\ j = 1 \tag{35}$$

$$\dot{X}_{F3} = A_3(X_{Fi}, U_{Fj}) + B_3(X_{Fi}, U_{Fj})U_{F3}$$

$$i = 1, 3;\ j = 1, 2 \tag{36}$$

where $X_{F1} = [\Theta, \Phi, \Psi]^T$, $U_{F1} = 0$, $X_{F2} = Q$, $U_{F2} = \Delta_e$, $X_{F3} = [W, P, R, V]^T$, and $U_{F3} = [\Delta_a, \Delta_T]^T$. This scheme, which differs from the one of Ref. 16 as far as controlled variables and tuning parameters are concerned, allows a stable NID control law to be derived. It neglects the derivatives of the aerodynamic forces (but not of the aerodynamic moments) with respect to the control surface deflections Δ_e, Δ_a, Δ_r and to the body angular rates P, Q, R. These force effects are small for the most current atmospheric vehicle configurations and are not the primary means of aerodynamic control, since the principal function of the control surface's deflection is to impart aerodynamic moments about the body axes. If the NID approach depends on these weak-force effects for control, either unrealistically large control deflections will be required for small vehicle position perturbation or the system will be destabilized by canceling the nonlinear equivalent of non-minimum-phase transmission zeros with unstable poles.[16] The practical control law is obtained by differentiating Θ, Φ, Ψ twice using the atmospheric vehicle triangular representation until the controls appear explicitly[4]:

$$\begin{pmatrix} \ddot{\Theta} \\ \ddot{\Phi} \\ \ddot{\Psi} \end{pmatrix} = \begin{pmatrix} A_\Theta \\ A_\Phi \\ A_\Psi \end{pmatrix} + \begin{pmatrix} B_\Theta^{\Delta_e} & B_\Theta^{\Delta_a} & B_\Theta^{\Delta_r} \\ B_\Phi^{\Delta_e} & B_\Phi^{\Delta_a} & B_\Phi^{\Delta_r} \\ B_\Psi^{\Delta_e} & B_\Psi^{\Delta_a} & B_\Psi^{\Delta_r} \end{pmatrix} \begin{pmatrix} \Delta_e \\ \Delta_a \\ \Delta_r \end{pmatrix} \tag{37}$$

The coefficients $A_{(\cdot)}$ and $B_{(\cdot)}$ are given in the Appendix. In contrast, From Eq. (33), the linear prescribed dynamics that control the NID loop is

$$\begin{pmatrix} \ddot{\Theta} \\ \ddot{\Phi} \\ \ddot{\Psi} \end{pmatrix} = -\begin{pmatrix} P_1^\Theta & 0 & 0 \\ 0 & P_1^\Phi & 0 \\ 0 & 0 & P_1^\Psi \end{pmatrix} \begin{pmatrix} \dot{\Theta} \\ \dot{\Phi} \\ \dot{\Psi} \end{pmatrix} - \begin{pmatrix} P_0^\Theta & 0 & 0 \\ 0 & P_0^\Phi & 0 \\ 0 & 0 & P_0^\Psi \end{pmatrix} \begin{pmatrix} \Theta - \bar{\Theta} \\ \Phi - \bar{\Phi} \\ \Psi - \bar{\Psi} \end{pmatrix} \tag{38}$$

The elements $P_k^{(\cdot)}$ that individually set the approximate response of the independent single-input, single-output (SISO) linear systems can be chosen according to the required flying qualities. For instance, if the tuning parameters are set for $P_1^{(\cdot)} = 1.4$ and $P_0^{(\cdot)} = 1$, a response time of about 1 s for all controlled loops will result. Obviously, a more refined pole allocation may be performed according to the vehicle capabilities and the desired flying qualities. This design assures good transient performances combined with the simplicity of the control law.

B. MPC Tracking Algorithm

MPC Mathematical Formulation

Because of the vehicle nonlinear dynamics, one must consider a model of the form

$$\dot{X}_F = f(X_F, U_F) + w \tag{39}$$

$$Y_F = g(X_F) + v \tag{40}$$

$$E(w^T w) = Q, \qquad E(v^T v) = R, \qquad E(w^T v) = 0 \tag{41}$$

The model of atmospheric turbulence[6,7,18] may be used to generate the w variable. The nonlinear model without noise (NLM) may be linearized with respect to $X_F(kT)$, $U_F(kT)$, where T is the linearization sampling period, to obtain a local linear model (LM):

$$\dot{x}_F = A_k x_F + B_k u_F \tag{42}$$

$$y_F = C_k x_F \tag{43}$$

The discretization of this internal model leads to the discrete-time local model (DTLM) used by the predictive algorithm. To keep the notation simple, the index F will be omitted:

$$x_{j+1} = F_k x_j + G_k u_j \tag{44}$$

$$y_j = C_k x_j \tag{45}$$

where

$$F_k = e^{A_k T}, \qquad G_k = \left(\int_0^\tau e^{A_k \tau} \, d\tau \right) B \tag{46}$$

The matrices F_k, G_k may be computed either using LM (A_k, B_k) or by an identification procedure[14] assuming that all of the states are measured. The prediction of the system output trajectory using the system current state information is given by[14,17]

$$\hat{y}(k+p) = y^*(k+p) + \sum_{i=1}^{p} h_{i,k} \Delta u(k+p-i) \qquad p = 1, P \tag{47}$$

where P is the prediction horizon, $y^*(k+p)$ represents the effect of the past inputs on future output predictions (the input values in the future are kept constant and equal to U_{k-1}), and $h_{i,k}$ denotes the step response coefficients [the contribution of the future manipulated variables $\Delta u(k) = u(k) - u(k-1)$ to the predicted output is represented by the sum in Eq. (47)]. Then

$$y^*(k+p) = C_k F_k^{P-1} x_{k-1} + h_{p,k} u_{k-1} \qquad p = 1, P \tag{48}$$

$$h_{p,k} = \sum_{i=1}^{p} C_k F_k^{i-1} G_k \qquad p = 1, P \tag{49}$$

Note that in Eq. (47) the predicted command is considered as its incremental value. Then, the matrix form of the prediction law is

$$\hat{Y} = H \Delta U + Y^* \tag{50}$$

where

$$\hat{Y} = [\hat{y}(k+p)] \qquad Y^* = [y^*(k+p)] \qquad p = 1, P$$

$$\Delta U = [u(k+i)] \qquad i = 1, M \tag{51}$$

$$H = \left(\begin{array}{cc|c} h_{1,k} & 0 & 0 \\ h_{2,k} & h_{1,k} & 0 \\ \hline h_{P,k} & h_{P,1,k} & h_{P-M+1,k} \end{array} \right) \tag{52}$$

One obtains the reference trajectory by modifying the desired one to accommodate the practical requirements and, possibly, the physical constraints of the controlled system.[14,17] The general form of the reference trajectory is

$$Y_{tr}(k+1) = E Y_{tr}(k) + (I - E) Y_d(k) \tag{53}$$

$$Y_{tr}(k) = Y(k) = [y_i(k)]_{i=1,N_{yc}} \tag{54}$$

with $Y_{tr}(\cdot)$ the reference trajectory vector of dimension N_{yc} (N_{yc} the number of controlled outputs), $Y_d^{(\cdot)} = [y_d(\cdot)]$ the desired trajectory vector, I the unit matrix, E a diagonal matrix $0 < E < I$, and $Y(\cdot)$ the current trajectory vector. The E matrix plays an important role in tracking rapidity: $E = 0$ denotes an instant pursuit; for $E = I$ the approach time tends to infinity. The E matrix selection concerns both the algorithm robustness and the tracking performances. Usually, as is the case in the present paper, one chooses $E = \text{diag}[\exp(-Tk/\tau)]$, where τ is the tracking time constant.

The main purpose of the predictive control is to force the system to follow the reference trajectory within the tolerance limits imposed by the performance criterion. To accomplish this task, the difference between the current and the reference trajectories must be minimized, avoiding meanwhile an excessive variation of the inputs. The performance criterion may be defined as

$$J = \min_{\Delta u(k+j),\ j=1,M} \sum_{p=k+I}^{k+p} \left\{ [\hat{y}(p) - y_d(p)]^T Q^2 [\hat{y}(p) - y_d(p)] + \Delta u^T (p-1) R^2 \Delta u(p-1) \right\} \tag{55}$$

where M is the number of nonzero computed commands [$\Delta u(k+M+1) = \cdots = \Delta u(k+P) = 0$] and $Q = \text{diag}[\gamma(i)]$, $R = \text{diag}[\lambda(i)]$.[12] Minimization of this criterion leads to the control law

$$\Delta U = (H^T Q^2 H + R^2)^{-1} H^T Q^2 (Y_d - \hat{Y}) \tag{56}$$

This result corresponds, in the particular case when $R = 0$, to the solution obtained by means of the generalized pseudoinverse.[14,17] After applying the current command, which is the first one computed, the algorithm must be updated, based on the current measurement, to preserve the closed-loop stability. This procedure consists in using the current measurement to estimate the state vector, if it is necessary, and to transfer the initial condition to the next computational step.

For the systems with incomplete state information, the nonaccessible state vector should be estimated as presented in Ref. 13. For every estimation procedure, the updating of the parameters of the discrete Kalman filters is done as in Ref. 19. For systems having a complete state information, the system output, $y^*(k+p)$, might be calculated using Eq. (48). The matrices F_k and G_k of DTLM can be built, for systems with complete state information, using an on-line recursive identification procedure.[14,17]

MPC Implementation

The practical implementation of the predictive control method, applied to a nonlinear and nonstationary system such as the atmospheric vehicle, assumes the accessibility of the state information. The vehicle equations of motion are presented in Sec. III, considering the controlled output vector $Y(k) = (\theta, h \mid \phi, \psi)^T$, as well as the desired one, $Y_d(k) = (\theta_d, h_d \mid \phi_d, \psi_d)^T$, characterizes both the longitudinal and lateral behaviors, where $h = -[H_D(kT + t) - H_D(kT)]$.

The control is performed separately, considering decoupled linear state and control vectors, i.e., for the longitudinal motion $x_{LN} = (q \;\; u \;\; w \;\; \theta)^T$ and $\delta_{LN} = (\delta_e, \delta_t)^T$ and for the lateral motion $x_{LT} = (p \;\; r \;\; v \;\; \varphi)^T$ and $\delta_{LT} = (\delta_a, \delta_r)^T$. Note that the longitudinal control δ_e is computed to minimize at the same time both differences $\theta_d - \theta$ and $h_d - h$. In this way a more precise vertical plane tracking is assured. The control δ_t is derived from the IKP algorithm. This applies for both conventional aircraft and helicopters. For the MPC implementation the state and control vector components are considered in their incremental form.

The data described in the previous section must be gathered and updated at the instant k. One can note that the algorithm initialization is made for an equilibrium condition. The evaluation of the

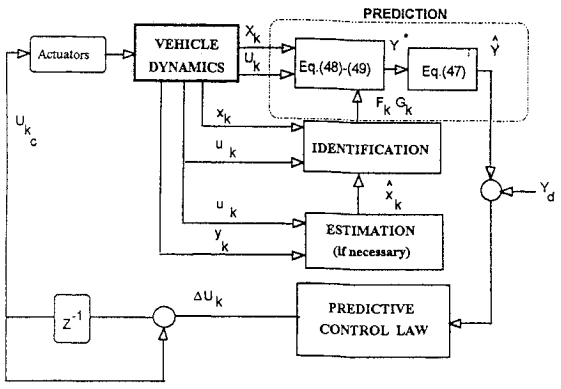

Fig. 4 MPC solution block diagram.

current control effects implies the identification of the DTLM, computation of the step response coefficients h_{ik} (using the matrices F_k and G_k), and evaluation of the controlled output prediction $\hat{Y}(k)$ and the H matrix. Minimization of the optimization criterion permits the computation of the best set of future commends, only the first then being applied. Differences from the preceding case occur in the nonaccessible state measurement. This implies the necessity of state estimation.[13] Then the state can be constructed using the measured and the estimated components. As in the previous case the first future computed command is applied at the updating time. The block diagram of the proposed algorithm, in the most general case, is presented in Fig. 4.

VI. Algorithm Performance Evaluation

The performances of the algorithms previously described are evaluated by means of a specialized computer-based simulation.[20]

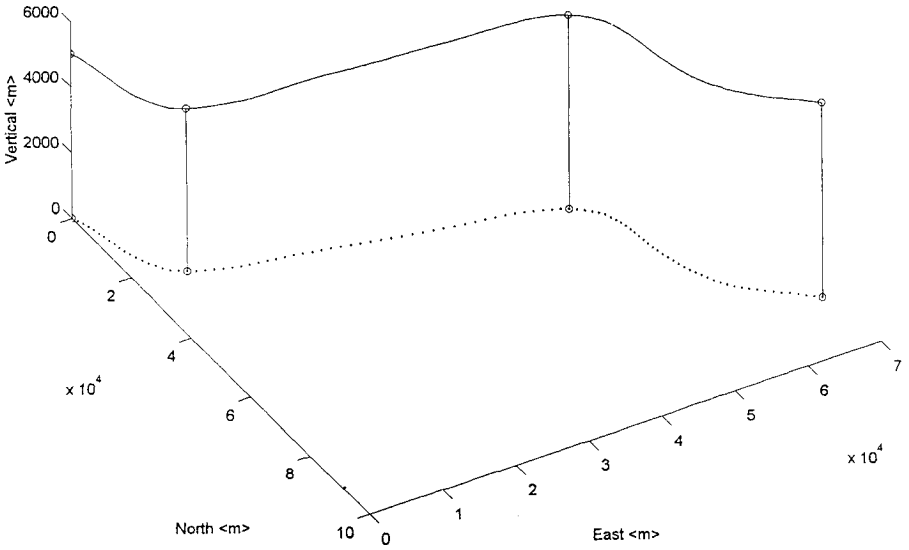

Fig. 5a Three-dimensional desired test trajectory.

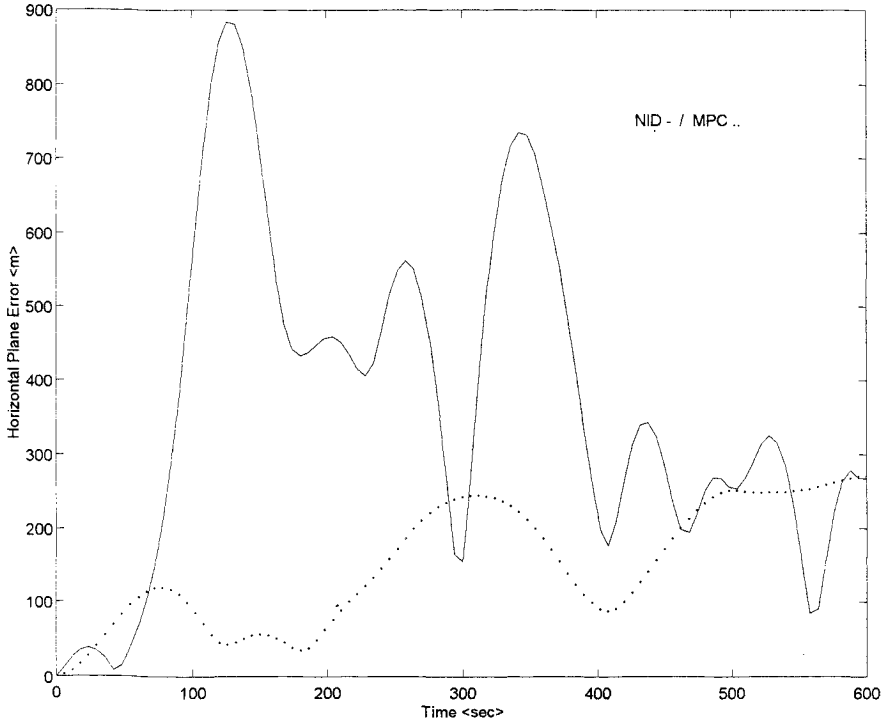

Fig. 5b Four-dimensional guidance: horizontal plane error vs time.

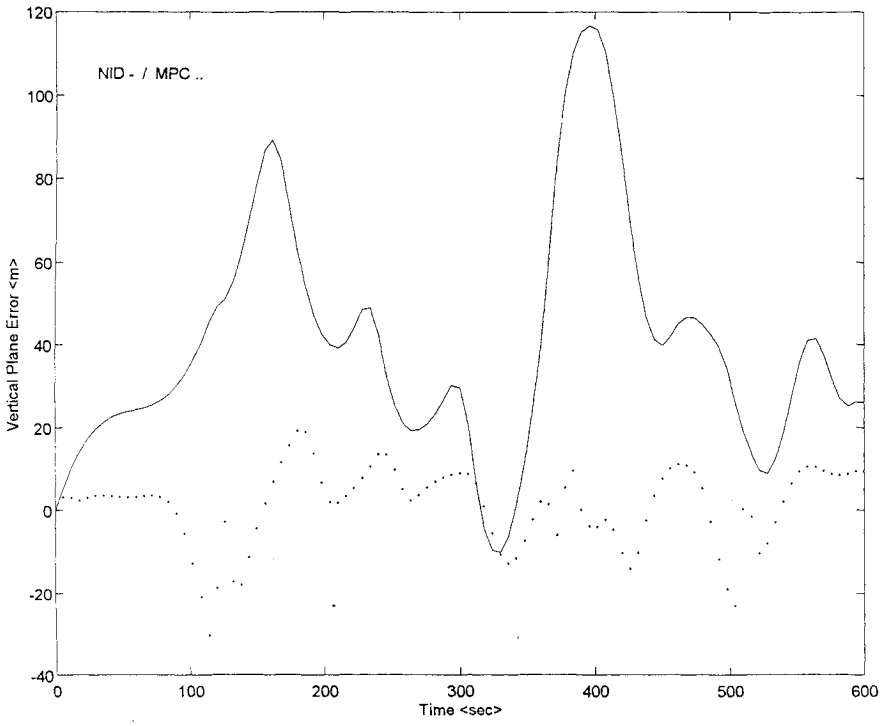

Fig. 5c Four-dimensional guidance: vertical plane error vs time.

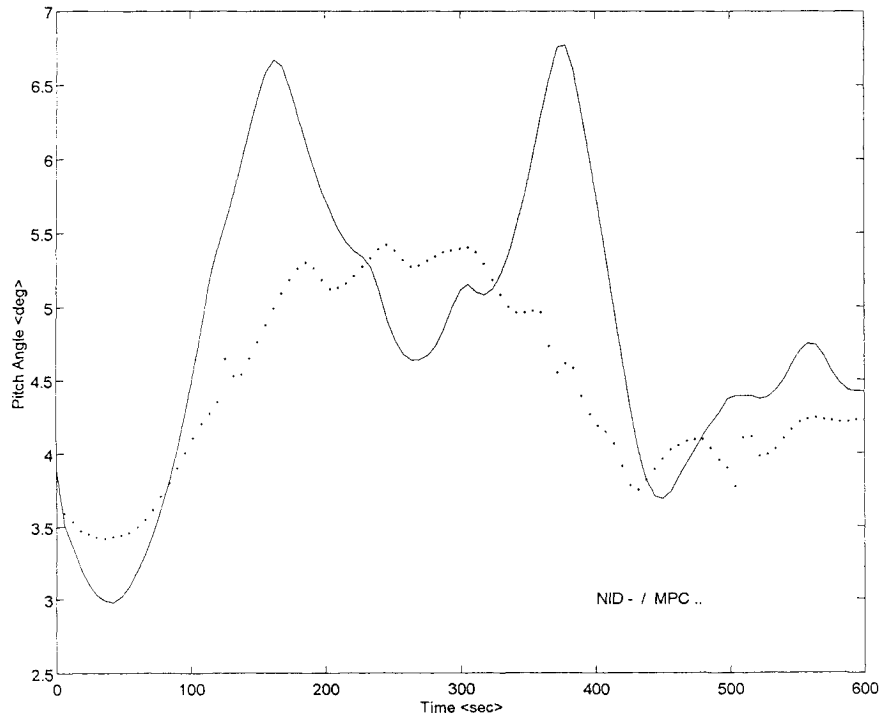

Fig. 5d Four-dimensional guidance: desired pitch attitude vs time.

The model of a conventional transport aircraft with rigid-body dynamics under the flat-Earth assumption has been simulated using the data from Ref. 8. To this end, a quasistatic aerodynamics linearization, a direct trim calculation, and first-order dynamics for the engine thrust and actuators were also considered with adequate limitations for displacements and rates. A model for atmospheric perturbation is used.[15,20]

A set of desired four-dimensional test trajectories defined by flight levels, waypoints, and estimated times of arrival has been used to verify the tracking performance. The parameters were tuned via simulation to minimize the tracking error. The NID gains of the slow time-scale controller have been established at $K_L = 0.1$ rad/m, $K_V = 2 \times 10^5$ rad/m, and the dynamics of the NID controller is defined by a damping ratio of 0.7 and a response time of 3 s. A possible set of MPC tuning parameter was presented in Ref. 13.

Figure 5 shows the results of a comparative NID/MPC simulation case that considers a desired test trajectory (Fig. 5a) generated by a cubic-spline interpolation over four waypoints from 5000 to 6000 m. Figures 5b and 5c show the tracking errors in the horizontal and vertical planes. The horizontal plane error (Fig. 5b) allows one to conclude the MPC tracking is decidedly better than the NID one but is more complex and expensive. For a specific application, an extensive set of simulations would be conducted to decide if the NID algorithm satisfies the particular requirements or an MPC algorithm is necessary. Figure 5c points out a maximum altitude tracking error

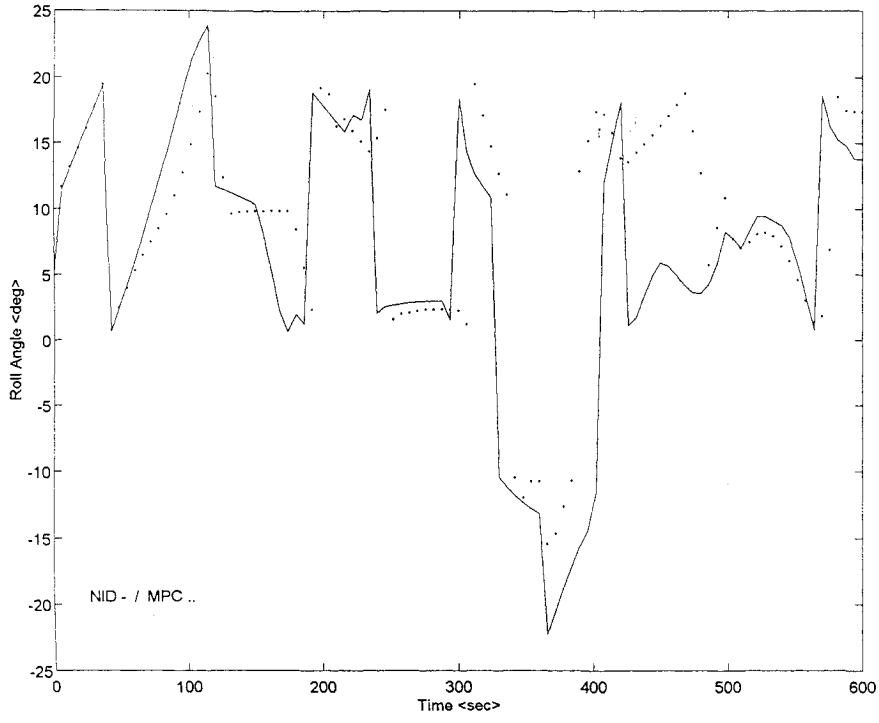

Fig. 5e Four-dimensional guidance: desired roll attitude vs time.

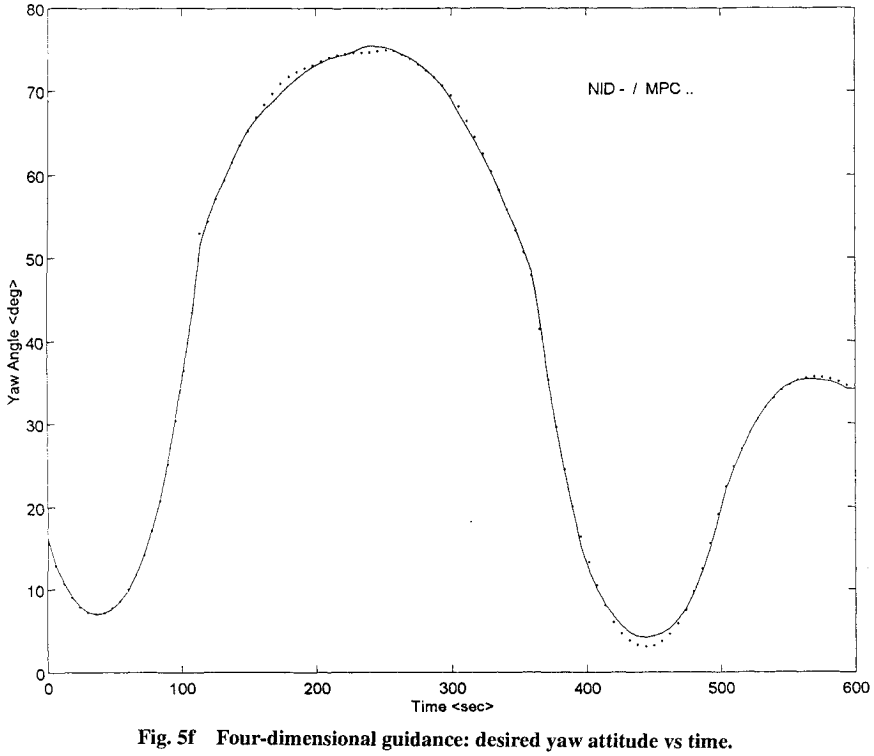

Fig. 5f Four-dimensional guidance: desired yaw attitude vs time.

of about 20 m in the case of the MPC algorithm (where the elevator command is computed to minimize the difference between the desired and the current altitude) and one of about 120 m in the case of the NID algorithm.

Figures 5d–5f allow for a comparison between the slow-time desired attitudes in the case of the NID or the MPC control. Note that for the same four-dimensional test trajectory the IKP algorithm values for the desired attitude and the thrust control are different (see Sec. IV). The pitch attitude is tracked by the NID algorithm to within 3 deg, the MPC algorithm assuring tracking to within 4 deg (as an average tracking between the pitch attitude and the altitude). The roll attitude is tracked to within 4 deg and the heading to within 2 deg in the case of the NID control. These values are 50% smaller in the case of the MPC control except for the pitch attitude. Note that good attitude tracking represents a good premise for a precise four-dimensional tracking.

VII. Conclusions

Drawing upon some recently developed control methods, a specific four-dimensional guidance algorithm was designed. The nonlinear inverse dynamics and the model predictive control strategies have been used to design an attitude guidance algorithm for an atmospheric vehicle using the inverse kinematics problem solution that converts the time-defined three-dimensional trajectory to the desired attitude to be tracked and the throttle command. According to the singular perturbation method, a time-scale separation between

the position and the attitude dynamics has been made to simplify the control task. This separation allows for a solution of the four-dimensional guidance using a control algorithm developed in two steps. In the first step the desired attitude is determined, whereas in the second step this attitude is tracked using either the nonlinear inverse dynamics or the model predictive control. The model predictive attitude control algorithm assures smooth and precise tracking, but it requires extensive computational capabilities that result in a difficult and expensive implementation. The nonlinear inverse attitude control algorithm assures good tracking performance, satisfying in general the most usual applications, while being less demanding computationally.

The resulting algorithm was tuned by simulation to assure the entire flight envelope performance in the case of a transport aircraft. The overall performance of the proposed guidance system has been demonstrated in a representative simulation that confirms the tracking effectiveness. Thus it appears that future autopilots could greatly benefit from implementation of the proposed algorithm for real-time guidance. Other facets of the problem justify further research: For instance, one should investigate the integration of the robust control methodologies into the design of that guidance algorithm.

Appendix: Expressions for Aircraft Coefficients

$$A_\Theta = A_2^2 - A_3^3 - A_\Theta^r$$

$$A_\Phi = A_3^2 + A_2^2 \sin\Phi \tan\Theta + A_3^3 \cos\Phi \tan\Theta - A_\Phi^r$$

$$A_\Psi = A_2^2 \sin\Phi \sec\Theta + A_3^3 \cos\Phi \sec\Theta - A_\Psi^r$$

$$A_\Theta^r = -\sec\Theta(Q\sin\Phi + R\cos\Phi)^2$$

$$A_\Phi^r = A_1^1 \sec\Theta\left(A_1^4 \sin\Theta + A_1^3\right)$$

$$A_\Psi^r = A_1^1 \sec\Theta\left(A_1^3 \sin\Theta + A_1^4\right)$$

$$A_1^1 = Q\cos\Phi - R\sin\Phi$$

$$A_1^2 = U\sin\Theta - V\cos\Theta\sin\Phi - W\cos\Theta\cos\Phi$$

$$A_1^3 = (Q\sin\Phi + R\cos\Phi)\sec\Theta$$

$$A_1^4 = P + (Q\sin\Phi + R\cos\Phi)\tan\Theta$$

$$A_2^1 = -RV + QW - g\sin\Theta - (X_a\sin\alpha - Z_a'\cos\alpha)/m$$

$$\alpha = \sin^{-1}(W/V)$$

$$X_w = \tfrac{1}{2}\rho V^2 S C_{x0} + K_{p1}\left(2Z_w^2/\rho V^2 S\right)$$

$$Z_w' = \tfrac{1}{2}\rho V^2 S\left(C_{z0} + C_{z\alpha}(W/V) + (c/2V^2)C_{z\alpha p}\dot{W} - (c/2V)C_{zq}Q\right)$$

$$A_2^2 = \left[J_{xz}(R^2 - P^2) + PR(I_z - I_x) + M_w'\right]/I_y$$

$$M_w' = \tfrac{1}{2}\rho V^2 Sc\left(C_{m0} + C_{m\alpha}(W/V) + (c/2V^2)C_{m\alpha p}\dot{W} + (c/2V)C_{mq}Q\right)$$

$$A_3^1 = -PV + QU + g\cos\Theta\cos\Phi - (X_a\sin\alpha + Z_a'\cos\alpha)/m$$

$$A_3^2 = \left(E_p' I_z + E_r' J_{xz}\right)/\left(I_x I_z - J_{xz}^2\right)$$

$$A_3^3 = \left(E_p' J_{xz} + E_r' I_x\right)/\left(I_x I_z - J_{xz}^2\right)$$

$$E_p' = J_{xz}PQ - (I_y - I_z)QR + L'$$

$$E_r' = -J_{xz}QR - (I_x - I_y)PQ + N'$$

$$L' = L_w'\cos\alpha - N_w'\sin\alpha$$

$$N' = L_w'\sin\alpha + N_w'\cos\alpha$$

$$L_w' = \tfrac{1}{2}\rho V^2 Sb(C_{l\beta}(V/V) + (b/2V)C_{lp}P + (b/2V)C_{lr}R)$$

$$N_w' = \tfrac{1}{2}\rho V^2 Sb(C_{n\beta}(V/V) + (b/2V)C_{np}P + (b/2V)C_{nr}R)$$

$$A_3^4 = -RU + WP + g\cos\Theta\cos\Phi - pV^2 SC_{m\beta}(V/mV)$$

$$B_\Theta^{\Delta_e} = B_{\Delta_e}^Q\cos\Phi, \qquad B_\Theta^{\Delta_a} = -B_{\Delta_a}^P\sin\Phi$$

$$B_\Theta^{\Delta_r} = -B_{\Delta_r}^R\sin\Phi$$

$$B_\Phi^{\Delta_e} = B_{\Delta_e}^Q\sin\Phi\tan\Theta, \quad B_\Phi^{\Delta_a} = B_{\Delta_a}^P + B_{\Delta_a}^R\cos\Phi\tan\Theta$$

$$B_\Phi^{\Delta_r} = B_{\Delta_r}^P + B_{\Delta_r}^R\cos\Phi\tan\Theta$$

$$B_\Psi^{\Delta_e} = B_{\Delta_e}^Q\sin\Phi\sec\Theta, \qquad B_\Psi^{\Delta_a} = B_{\Delta_a}^R\cos\Phi\sec\Theta$$

$$B_\Psi^{\Delta_r} = B_{\Delta_r}^R\sin\Phi\sec\Theta$$

$$B_{\Delta_r}^Q = \rho V^2 ScC_{m\delta_e}/2I_y$$

$$B_{\Delta_a}^P = B_{\Delta_a}^{'P} + B_{\Delta a}^{''P}$$

$$B_{\Delta_a}^{'P} = \rho V^2 SbI_z\left(C_{l\delta_a}\cos\alpha - C_{n\delta_a}\sin\alpha\right)/\left(I_x I_z - J_{xz}^2\right)$$

$$B_{\Delta a}^{''P} = \rho V^2 SbJ_{xz}\left(C_{l\delta_a}\sin\alpha + C_{n\delta_a}\cos\alpha\right)/\left(I_x I_z - J_{xz}^2\right)$$

$$B_{\Delta_r}^P = B_{\Delta_r}^{'P} + B_{\Delta_r}^{''P}$$

$$B_{\Delta_r}^{'P} = \rho V^2 SbI_z\left(C_{l\delta_r}\cos\alpha - C_{n\delta_r}\sin\alpha\right)/\left(I_x I_z - J_{xz}^2\right)$$

$$B_{\Delta_r}^{'P} = \rho V^2 sbJ_{xz}\left(C_{l\delta_r}\sin\alpha + C_{n\delta_r}\cos\alpha\right)/\left(I_x I_z - J_{xz}^2\right)$$

$$B_{\Delta_a}^R = B_{\Delta_a}^{'R} + B_{\Delta_a}^{''R}$$

$$B_{\Delta_a}^{'R} = \rho V^2 SbJ_{xz}\left(C_{l\delta_a}\cos\alpha - C_{n\delta_a}\sin\alpha\right)/\left(I_x I_z - J_{xz}^2\right)$$

$$B_{\Delta_a}^{''R} = \rho V^2 SbI_x\left(C_{l\delta_a}\sin\alpha + C_{n\delta_a}\cos\alpha\right)/\left(I_x I_z - J_{xz}^2\right)$$

$$B_{\Delta_r}^R = B_{\Delta_r}^{'R} + B_{\Delta_r}^{''R}$$

$$B_{\Delta_r}^{'R} = \rho V^2 SbJ_{xz}\left(C_{l\delta_r}\cos\alpha - C_{n\delta_r}\sin\alpha\right)/\left(I_x I_z - J_{xz}^2\right)$$

$$B_{\Delta_r}^{''R} = \rho V^2 SbI_x\left(C_{l\delta_r}\sin\alpha - C_{n\delta_r}\cos\alpha\right)/\left(I_x I_z - J_{xz}^2\right)$$

References

[1]Heiges, M. W., Menon, P. K. A., and Schrage, D. P., "Synthesis of a Helicopter Full-Authority Controller," *Journal of Guidance, Control, and Dynamics*, Vol. 15, No. 1, 1992, pp. 222–227.

[2]Snell, S. A., Enns, D. F., and Garrard, W. L., "Nonlinear Inversion Control for a Supermaneuverable Aircraft," *Journal of Guidance, Control, and Dynamics*, Vol. 15, No. 4, 1992, pp. 976–984.

[3]Menon, P. K. A., Badget, M. E., and Walker, R. A., "Nonlinear Flight Test Trajectory Controllers for Aircraft," *Journal of Guidance, Control, and Dynamics*, Vol. 10, No. 1, 1987, pp. 67–72.

[4]Stiharu-Alexe, I., "On Nonlinear Inverse Dynamics Control in 4D Aircraft Guidance," Grenoble Automatics Lab., Rept. 92-127, Grenoble, France, 1992.

[5]Kato, O., and Sugiura, I., "An Interpretation of Airplane General Motion and Control Inverse Problem," *Journal of Guidance, Control, and Dynamics*, Vol. 9, No. 2, 1986, pp. 198–204.

[6]Etkin, B., *Dynamics of Atmospheric Flight*, Wiley, New York, 1982.

[7]McRuer, D., Ashkenas, L., and Graham, D., *Aircraft Dynamics and Automatic Control*, Princeton Univ. Press, Princeton, NJ, 1973.

[8]Wanner, J. C., "Dynamique du vol et pilotage des avions," ONERA Paper, 1983.

[9]Stiharu-Alexe, I., and Stiharu-Alexe, C., "A Full-Authority 4D Guidance Algorithm for Conventional Aircraft," *Proceedings of ACC'93 Conference*, San Francisco, CA, 1993, pp. 2561–2566.

[10]Reid, J. C., Chafin, D. E., and Silverthorn, J. T., "Output Predictive Control: Precision Tracking with Applications to Terrain Following," *Journal of Guidance and Control*. Vol. 4, No. 3, 1981, pp. 463–469.

[11]Morari, M., Economou, C. E., Garcia, C. E., and Holt, B. R., "Internal Model Control Theory and Applications," *Proceedings of American Control Conference*, San Diego, CA, 1984, pp. 532–543.

[12]Clarke, D. W., Tuffs, P. S., and Mothandi, C., "Generalized Predictive Control," *Automatica*, Vol. 23, 1987, pp. 137–160.

[13]Stiharu-Alexe, I., and O'Shea, J., "A Predictive Algorithm for 4D Tracking by Autopilots," Grenoble Automatics Lab., Rept. 92-151, CORS'94 Optimization Days, Transportation and Logistics, Montreal, 1994.

[14]Stiharu-Alexe, I., "Predictive Control for 4D Guidance," *Proceedings of SPIE Conference*, Vol. 1482, *Acquisition, Tracking, and Pointing V*, Orlando, FL, 1991, pp. 491–501.

[15]Singh, S. W., "Decoupling with Nearly Singular I-O Maps and Control of Aircraft," *Proceedings of the IEEE Twenty-Seventh Conference on Decision and Control* (Austin, TX), Inst. of Electrical and Electronics Engineers, 1988, pp. 706–711.

[16]Lane, S. H., and Stengel, R. F., "Flight Control Design Using Nonlinear Inverse Dynamics," *Proceedings of American Control Conference*, 1988, pp. 587–596.

[17]Stiharu-Alexe, L., and Stiharu-Alexe, C., "On Load Factor Constraints in Model Predictive Control," *Preprints of IFAC International Symposium on Adaptive Control and Signal Processing*, Grenoble, 1992, pp. 234–245.

[18]Anon., MIL-F-8785 B (ASG), "Military Specification Flying Qualities of Piloted Airplanes," 1969.

[19]Astrom, J. K., and Wittermark, B., *Computer Controlled Systems: Theory and Design*, Prentice–Hall, Englewood Cliffs, NJ, 1990.

[20]Stiharu-Alexe, I., Stiharu-Alexe, C., and Constantinescu, C., "ACAV Integration of the Simulation in the Control Analysis and Design of Atmospheric Vehicle Autopilots," Grenoble Automatics Lab., Rept. 92-148, Grenoble, France, 1993.